Journal of Organometallic Chemistry 751 (2014) 475–481

Contents lists available at ScienceDirect

Journal of Organometallic Chemistry

journal homepage: www.elsevier.com/locate/jorganchem

Facile cleavage of phenyl groups from $BiPh_3$ in its reactions with $Os_3(CO)_{10}(NCMe)_2$ and evidence for localization of π-bonding in a bridging benzyne ligand

Richard D. Adams*, Yuwei Kan, Qiang Zhang

Department of Chemistry and Biochemistry, University of South Carolina, Columbia, SC 29208, USA

ARTICLE INFO

Article history:
Received 23 May 2013
Received in revised form
4 July 2013
Accepted 9 July 2013

Keywords:
Phenyl cleavage
Osmium cluster
Bismuth
Benzyne

ABSTRACT

Three new compounds were obtained from the reaction of $Os_3(CO)_{10}(NCMe)_2$, **1** with $BiPh_3$ in a methylene chloride solution at reflux. These have been identified as $Os_3(CO)_{10}(\mu_3\text{-}C_6H_4)$, **3**, $Os_3(CO)_{10}Ph(\mu\text{-}\eta^2\text{-}O{=}CPh)$, **4**, and $HOs_6(CO)_{20}(\mu\text{-}\eta^2\text{-}C_6H_4)(\mu_4\text{-}Bi)$, **6**. Two other products $Os_2(CO)_8(\mu\text{-}BiPh)$, **2**, and $HOs_5(CO)_{18}(\mu\text{-}\eta^2\text{-}C_6H_4)(\mu_4\text{-}Bi)$, **5** were obtained previously from the reaction of $Os_3(CO)_{11}(NCMe)$ with $BiPh_3$. Cleavage of the phenyl groups from the $BiPh_3$ was the dominant reaction pathway and two of the products **3** and **4** contain rings but no bismuth. Each of the new compounds was characterized structurally by single-crystal X-ray diffraction methods. Compound **3** contains a triply-bridging benzyne (C_6H_4) ligand that exhibits a pattern of alternating long and short C–C bonds that can be attributed to partial localization of the π-bonding in the C_6 ring. The localization in the π-bonding in the ring is supported by DFT calculations. Compound **4** contains a triangular cluster of three osmium atoms with a bridging benzoyl ligand and a terminally coordinated phenyl ligand. Compound **6** contains six osmium atoms divided into two groups of four and two and the two groups are linked by a spiro-bridging bismuth atom. The group of two osmium atoms contains a bridging C_6H_4 ligand. When heated, compound **4** was converted into **3** and the compound $Os_3(CO)_{10}(\mu\text{-}\eta^2\text{-}O{=}CPh)_2$, **7**. Compound **7** contains two bridging benzoyl ligands.

1. Introduction

The cleavage of phenyl groups from the triphenylphosphine, PPh_3, in its reactions with triosmium dodecacarbonyl goes back to some of the very first reactions of this complex that were studied [1,2]. Cleavage of phenyl groups from $AsPh_3$ and $SbPh_3$ in triosmium carbonyl complexes is also facile [3,4]. Recently, complexes containing transition metal–bismuth bonds have attracted attention [5,6]. Transition metal–bismuth catalysts have been shown to exhibit high activity and selectivity for the oxidation and ammoxidation of hydrocarbons [7–9]. We have recently reported the synthesis of dirhenium carbonyl complexes containing $SbPh_2$ and $BiPh_2$ ligands by the cleavage of phenyl rings from $SbPh_3$ and $BiPh_3$ in their reactions with $Re_2(CO)_8[\mu\text{-}\eta^2\text{-}C(H){=}C(H)Bu^n](\mu\text{-}H)$, Eq. (1) [10]–(2) [11]. These products have been shown to be good catalysts for the ammoxidation of 3-picoline to 3-cyanopyridine [12].

We have also shown that phenyl groups are readily cleaved from $BiPh_3$ in its reaction with $Os_3(CO)_{11}(NCMe)$, Scheme 1 [13]. In fact, only one product, $Os_2(CO)_8(\mu\text{-}BiPh)$, contained any phenyl groups bonded to a Bi atom. Products containing phenyl groups or ligands derived from them, such as C_6H_4 and PhCO, were abundant.

In this follow up study, we have now investigated the reaction of $BiPh_3$ with $Os_3(CO)_{10}(NCMe)_2$, **1**. These studies have yielded yet another new osmium–bismuth complex as well as some new osmium carbonyl complexes containing phenyl, benzoyl and benzyne ligands derived from the phenyl groups that were cleaved from the $BiPh_3$. Most interestingly, a high resolution structure analysis of one of the new products $Os_3(CO)_{10}(\mu_3\text{-}C_6H_4)$, **3** which contains a triply-bridging benzyne ligand shows a distinct pattern of long and short C–C bonds around the ring of the benzyne ligand. Molecular orbitals for **3** were obtained by density functional theory (DFT) calculations and indicate that this bonding pattern can be attributed to a partial localization of the π-bonding in the ring which is enhanced at the shorter C–C bonds. The results of these studies are reported herein.

* Corresponding author.
E-mail address: Adamsrd@mailbox.sc.edu (R.D. Adams).

0022-328X/$ – see front matter © 2013 Elsevier B.V. All rights reserved.
http://dx.doi.org/10.1016/j.jorganchem.2013.07.027

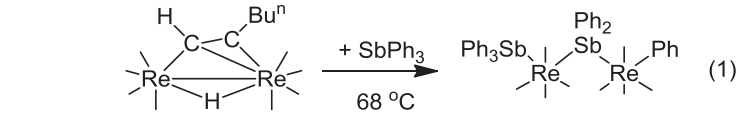

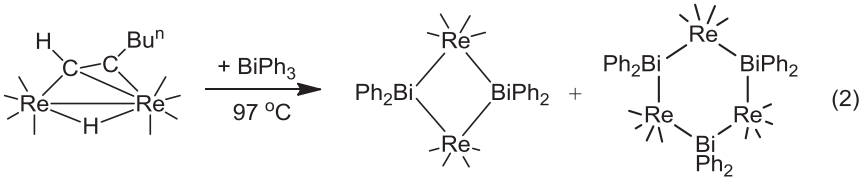

2. Experimental section

2.1. General data

Reagent grade solvents were dried by the standard procedures and were freshly distilled under nitrogen prior to use. Unless indicated otherwise, all reactions were performed under an atmosphere of nitrogen. Infrared spectra were recorded on a Thermo Nicolet Avatar 360 FT-IR spectrophotometer. ^{1}H NMR spectra were recorded on a Varian Mercury 300 spectrometer operating at 300.1 MHz. Mass spectral (MS) measurements were performed by a direct-exposure probe by using electron impact ionization (EI) on a VG 70S instrument. $Os_3(CO)_{12}$ was purchased from STREM. $BiPh_3$ was purchased from Alfa Aesar and was used without further purification. $Os_3(CO)_{10}(NCMe)_2$ was prepared according to the previously reported procedure [14]. Product separations were performed by TLC in open air on Analtech 0.25 mm or 0.5 mm silica gel 60 Å F_{254} glass plates.

2.2. Reactions of $Os_3(CO)_{10}(NCMe)_2$ with $BiPh_3$

A 52.3 mg (0.0561 mmol) amount of $Os_3(CO)_{10}(NCMe)_2$, **1** was dissolved in 30 mL of methylene chloride in a 100 mL three neck flask. To this solution was added 8.3 mg (0.0187 mmol) of $BiPh_3$. The solution was heated to reflux for 2 h. After cooling, the solvent was removed *in vacuo*, and the products were isolated by TLC by using an 8/1 hexane/methylene chloride elution solvent mixture to yield in order of elution: 1.9 mg of pale yellow $Os_2(CO)_8(\mu$-BiPh) [13], **2** (2.5% yield); 1.9 mg of yellow $Os_3(CO)_9(\mu$-CO)(μ_3-C_6H_4), **3** (3.6% yield); 6.5 mg of orange $PhOs_3(CO)_{10}(\mu$-η^2-O=CPh), **4** (11% yield); 5.2 mg of orange $HOs_5(CO)_{18}(\mu$-η^2-$C_6H_4)(\mu_4$-Bi) [13], **5** (8.9% yield); 7.9 mg of $HOs_6(CO)_{20}(\mu$-η^2-$C_6H_4)(\mu_4$-Bi), **6** (14% yield). Spectral data for **3**: IR νCO (cm^{-1} in hexane): 2099(vw), 2082(*w*), 2077(*w*), 2060(vs), 2024(s), 2012(s), 1998(*w*), 1983(vw), 1844(*w*). ^{1}H NMR (CD_2Cl_2, δ in ppm) at 25 °C: δ = 7.65 (m, 2H, C_6H_4), δ = 6.72 (m, 2H, C_6H_4). Mass Spec. EI/MS *m*/*z*. 928 (M^+). Spectral data for **4**. IR νCO (cm^{-1} in methylene chloride): 2111(m), 2096(*w*), 2059(vs), 2027(s),

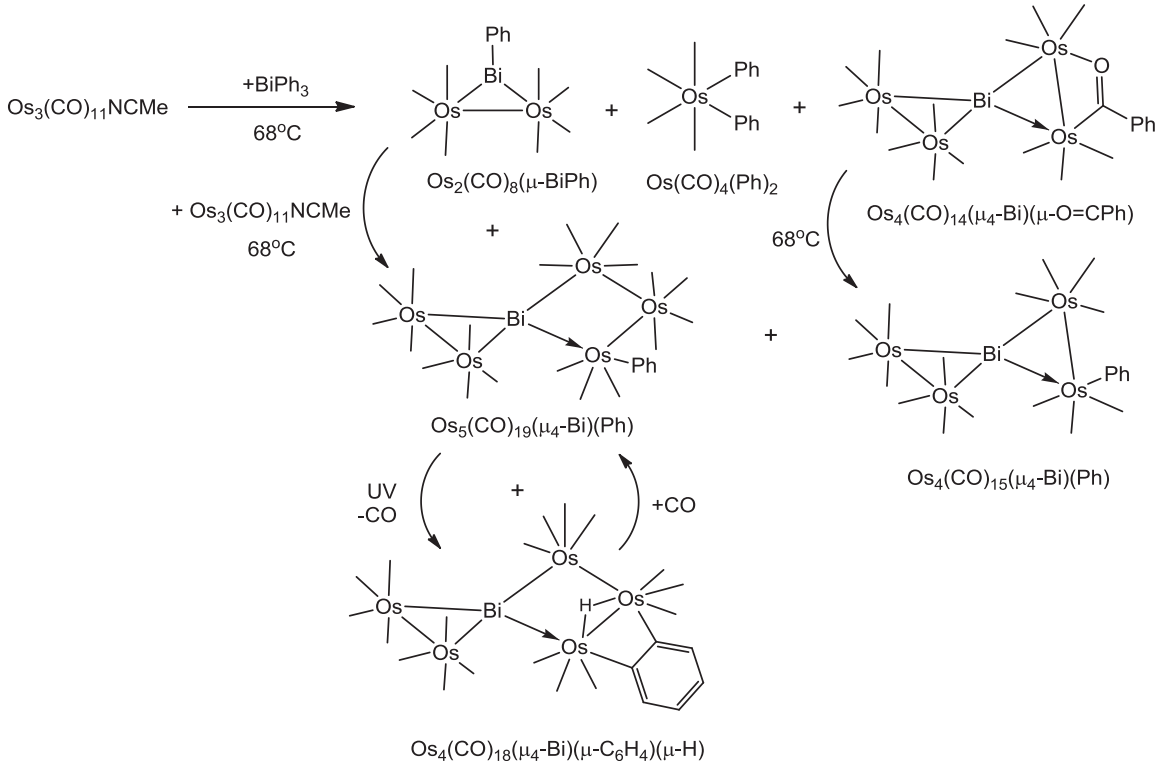

Scheme 1.

2003(m), 1986(m), 1942(*w*). ^{1}H NMR (CD_2Cl_2, δ in ppm) at 25 °C: $\delta = 7.22–7.84$ (m, 10H, Ph). EI/MS *m*/*z*. 1034 (M^+). Spectral data for **6**. IR *v*CO (cm^{-1} in hexane): 2126(*w*), 2089(m), 2082(m), 2073(s), 2056(*w*), 2044(vs), 2020(m), 2015(m), 2009(m), 2850(*w*). ^{1}H NMR (CD_2Cl_2, δ in ppm) at 25 °C: $\delta = 6.59–7.08$ (m, 4H, C_6H_4), $\delta = -14.54$ (s, hydride). EI/MS *m*/*z*. 1988 (M^+).

3. Thermal transformations of 4

A 7.4 mg (0.0072 mmol) amount of **4** was dissolved in 10 mL of hexane in a 50 mL three neck flask. The solution was heated up to reflux for 5 h. After cooling, the solvent was removed *in vacuo*, and the products were then isolated by TLC by using a 6/1 hexane/methylene chloride elution solvent mixture to yield in order of elution: 0.7 mg of **3** (10.5% yield); 3.2 mg of $Os_3(CO)_{10}(\mu\text{-}\eta^2\text{-}O{=}CPh)_2$, **7** [15] (42% yield). Spectral data for **7**: IR *v*CO (cm^{-1} in hexane): 2099(*w*), 2068(vs), 2048(m), 2016(vs), 2005(s), 1998(m), 1989(*w*), 1983(m), 1975(*w*), 1954(vw). Mass Spec. EI/MS *m*/*z*. 1062 (M^+).

3.1. Crystallographic analyses

Yellow single crystals of **3** and orange single crystals of **4** suitable for X-ray diffraction analysis were obtained by slow evaporation of solvent from solutions in hexane/methylene chloride solvent mixtures at −30 °C. Dark green single crystals of **6** suitable for X-ray diffraction analyses was obtained by slow evaporation of solvent from a solution of the pure compound in a hexane/methylene chloride solvent mixture at room temperature. Yellow single crystals of **7** suitable for X-ray diffraction analyses was obtained by slow evaporation of solvent from solutions in hexane solvent mixtures at −30 °C. Each data crystal was glued onto the end of a thin glass fiber. X-ray diffraction intensity data were measured by using a Bruker SMART APEX CCD-based diffractometer by using Mo Kα radiation ($\lambda = 0.71073$ Å). The raw data frames were integrated with the SAINT + program by using a narrow-frame integration algorithm [16]. Corrections for Lorentz and polarization effects were also applied with SAINT+. An empirical absorption correction based on the multiple measurement of equivalent reflections was applied using the program SADABS [16]. All structures were solved by a combination of direct methods and difference Fourier syntheses, and refined by full-matrix least-squares on F^2 by using the SHELXTL software package [17]. All non-hydrogen atoms were refined with anisotropic thermal parameters. The hydride ligand in compound **6** was refined on its positional parameters with a fixed isotropic thermal parameter. Compound **3** crystallized in orthorhombic system. The space group *P*na2_1 was indicated by the systematic absences in the data and confirmed by the successful solution and refinement for the structure. Efforts to solve the structure of **3** in the alternative centrosymmetric space group *P*nma were unsuccessful. Compounds **4**, **6** and **7** crystallized in monoclinic system. The space groups *P*2_1/c in compound **4** and *P*2_1/n for compounds **6** and **7** were uniquely identified by the systematic absences in the data and were subsequently confirmed by the successful solutions and refinements for the structures in each case. Crystal data, data collection parameters, and results of these analyses are listed in Table 1.

3.2. Computational details

Density functional theory (DFT) calculations were performed with the Amsterdam Density Functional (ADF) suite of programs [18] by using the PBEsol functional [19] with Slater-type valence quadruple-ζ + 4 polarization function, relativistically optimized (QZ4P) basis sets for osmium and valence triple-ζ + 2 polarization function (TZ2P) basis sets for carbon, oxygen, and hydrogen atoms with small frozen cores and a scalar relativistic ZORA (Zeroth-Order Regular Approximation) correction. The molecular orbitals for **3** and their energies were determined by a geometry-optimized gas-phase calculation that was initiated with the structure as found in the solid state. Electron densities at the bond critical points around the C_6 ring were calculated by using the Bader Quantum Theory of Atoms In a Molecule (QTAIM) model and the AIMAll software package [20,21].

Table 1
Crystallographic data for compounds 3, 4, 6 and 7.

Compound	**3**	**4**	**6**	**7**
Empirical formula	$Os_3O_{10}C_{16}H_4$	$Os_3O_{11}C_{23}H_{10}$	$Os_6BiO_{17}C_{29}H_{10}$	$Os_3O_{12}C_{24}H_{10}$
Formula weight	926.79	1032.91	1987.48	1060.92
Crystal system	Orthorhombic	Monoclinic	Monoclinic	Monoclinic
Lattice parameters				
a (Å)	13.9465(3)	10.9741(10)	9.6005(4)	16.766(3)
b (Å)	8.9230(2)	28.833(3)	24.3314(10)	9.4626(14)
c (Å)	15.2811(3)	8.4711(8)	16.4283(7)	16.991(3)
α (deg)	90.00	90.00	90.00	90
β (deg)	90.00	110.460(2)	102.0420(10)	99.243(3)
γ (deg)	90.00	90.00	90.00	90
V (Å^3)	1901.65(7)	2511.3(4)	3753.1(3)	2660.6(7)
Space group	*P*na2_1, no.33	*P*2_1/c, no.14	*P*2_1/n, no.14	*P*2_1/n, no.14
Z value	4	4	4	4
ρ_{calc} (g/cm^3)	3.237	2.732	3.517	2.649
μ (Mo K$_\alpha$) (mm^{-1})	20.048	15.200	24.977	14.354
Temperature (K)	294(2)	294(2)	294(2)	294(2)
$2\Theta_{max}$ (°)	56.06	50.06	50.06	50.06
No. Obs. ($I > 2\sigma(I)$)	3363	4429	6624	4689
No. Parameters	263	334	475	352
Goodness of fit GOF[a]	1.035	1.070	1.090	1.071
Max. shift in cycle	0.001	0.000	0.001	0.001
Residuals[a]: R1; wR2	0.0190, 0.0326	0.0423, 0.0759	0.0637, 0.1201	0.0368, 0.0793
Absorption	Multi-scan	Multi-scan	Multi-scan	Multi-scan
Correction, Max/min	1.000/0.749	1.000/0.703	1.000/0.523	1.000/0.646
Largest peak in Final Diff. Map (e−/Å^3)	0.496	1.369	2.935	1.387

GOF = $[\Sigma_{hkl} w\,(|F_{obs}| - |F_{calc}|)^2/(n_{data} - n_{vari})]^{1/2}$.

[a] $R = \Sigma_{hkl}(||F_{obs}| - |F_{calc}||)/\Sigma_{hkl}|F_{obs}|$; $R_w = [\Sigma_{hkl} w(|F_{obs}| - |F_{calc}|)^2/\Sigma_{hkl} wF^2_{obs}]^{1/2}$; $w = 1/\sigma^2(F_{obs})$.

4. Results

Five products: $Os_2(CO)_8(\mu\text{-BiPh})$ [13], **2** (2.5% yield), $Os_3(CO)_{10}(\mu_3\text{-}C_6H_4)$–, **3** (3.6% yield), $Os_3(CO)_{10}Ph(\mu\text{-}\eta^2\text{-O}{=}CPh)$, **4** (11% yield), $HOs_5(CO)_{18}(\mu\text{-}\eta^2\text{-}C_6H_4)(\mu_4\text{-Bi})$ [13], **5** (8.9% yield) and $HOs_6(CO)_{20}(\mu\text{-}\eta^2\text{-}C_6H_4)(\mu_4\text{-Bi})$, **6** (14% yield) were obtained all in low yields from the reaction of **1** with $BiPh_3$ in a methylene chloride solution at reflux for 2 h. Three of the products, **3**, **4** and **6** are new and were characterized by a combination of IR, NMR, mass spec and single-crystal x-ray diffraction analyses. Compounds **2** and **5** were obtained previously from the reaction of $Os_3(CO)_{11}(NCMe)$ with $BiPh_3$ [13].

An ORTEP diagram of the molecular structure of **3** is shown in Fig. 1. Compound **3** contains three osmium atoms, nine linear terminal carbonyl ligands, one asymmetrical bridging carbonyl ligand and a triply-bridging C_6H_4 benzyne ligand. Compound **3** is related to the family of compounds $Os_3(CO)_9(\mu_3\text{-}C_6H_3R)\text{-}(\mu\text{-H})_2$, R = H, CH_3, Cl, $HC_2(H)Ph$, that was reported by Johnson and Lewis many years ago [22]. The primary difference between **3** and the Johnson–Lewis compounds is that **3** has ten CO ligands and no hydride ligands, while the Johnson–Lewis compounds have nine CO ligands and two bridging hydride ligands. The three osmium–osmium bond distances in **3** are Os(1)–Os(2) = 2.8526(3) Å, Os(1)–Os(3) = 2.7631(4) Å and Os(2)–Os(3) = 2.7506(4) Å in length. By contrast, $Os_3(CO)_9(\mu_3\text{-}C_6H_4)\text{-}(\mu\text{-H})_2$ has two long Os–Os bonds, 3.026(2) [3.041(2)] Å, 2.866(2) [2.849(2)] Å and one shorter one, 2.751(2) [2.751(2)] Å [20]. The two long bonds in $Os_3(CO)_9(\mu_3\text{-}C_6H_4)\text{-}(\mu\text{-H})_2$ can be attributed to effects of the hydride ligands that bridge those bonds [23]. The bridging carbonyl ligand in **3**, C(14)–O(14), is slightly asymmetrically coordinated, Os(1)–C(14) = 2.104(8) Å, Os(2)–C(14) = 2.243(7) Å. The formal C–C triple bond of the benzyne ring in **3** is coordinated in the di-σ+π parallel coordination **A** that is well established for triply-bridging alkyne ligands [24]. Formally, the benzyne ligand in **3** serves as a 4-electron donor.

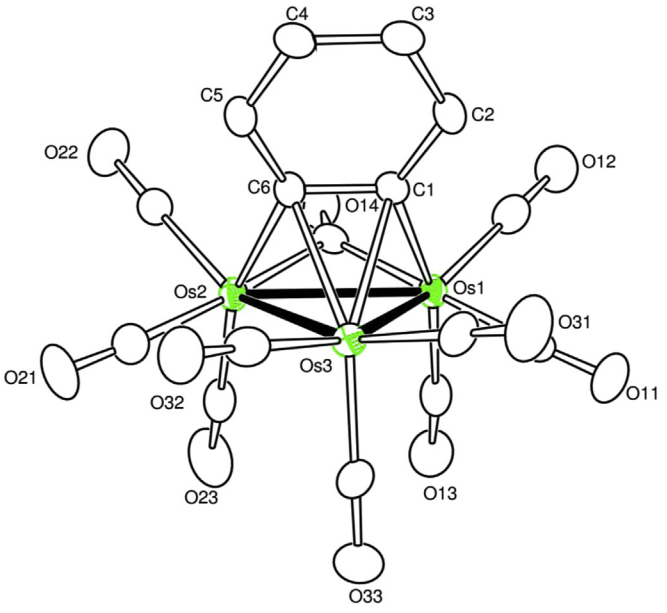

Fig. 1. An ORTEP diagram of the molecular structure of $Os_3(CO)_9(\mu\text{-CO})(\mu_3\text{-}C_6H_4)$, **3** showing 40% thermal ellipsoid probability. The hydrogen atoms are omitted for clarity. Selected interatomic bond distances (Å) are as follow: Os(1)–Os(2) = 2.8526(3), Os(1)–Os(3) = 2.7631(4), Os(2)–Os(3) = 2.7506(4), Os(1)–C(1) = 2.119(8), Os(3)–C(1) = 2.335(6), Os(2)–C(6) = 2.121(7), Os(3)–C(6) = 2.316(7), Os(1)–C(14) = 2.104(8), Os(2)–C(14) = 2.243(7), C(1)–C(6) = 1.406(9), C(1)–C(2) = 1.438(9), C(2)–C(3) = 1.375(10), C(3)–C(4) = 1.405(10), C(4)–C(5) = 1.361(10), C(5)–C(6) = 1.428(10).

Overall, the cluster has 48 valence electrons and each of the osmium atoms achieves an 18-electron configuration in the presence of three Os–Os bonds.

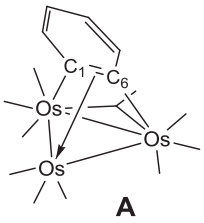

A

The C(1)–C(6) distance is 1.406(9) Å in length. Because of the high quality of this structure analysis, a pattern of alternating long and short C–C bond distances observed about the C_6 ring, C(1)–C(2) = 1.438(9) Å, C(2)–C(3) = 1.375(10) Å, C(3)–C(4) = 1.405(10) Å, C(4)–C(5) = 1.361(10) Å and C(5)–C(6) = 1.428(10) Å, seems to be a true effect. A similar pattern was observed for the quadruply-bridging benzyne ligand found in the complex $Ru_5((\mu\text{-CO})_2(CO)_{11}(\mu_3\text{-}\eta^3\text{-}SC_{12}H_8)\text{-}(\mu_4\text{-}C_6H_4)(\mu_5\text{-S})$ [25]. The alternating pattern observed in the structure of the ring found in **3** can be explained by partial localizations in the π–bonding in the C_6 ring induced by interruption in the delocalization of the π–bonding at the C(1)–C(6) bond due to the coordination of these atoms to the metal atoms. This occurs by utilizing the out of plane π-orbitals of the ring as illustrated by the bonding model shown in structure **A**. This idea was supported by geometry-optimized density functional theory (DFT) calculations that were performed on the structure of **3**. Two of the key molecular orbitals in **3**, the HOMO and the HOMO-2, are shown in Fig. 2. They display a clear pattern of enhanced π-bonding between the two pairs of atoms, C(2)–C(3) and C(4)–C(5), which exhibit the shortest of the C–C ring bond distances. Selected bond distances obtained from the crystal structure determination are compared with the corresponding values obtained from the geometry-optimized DFT calculations in Table 2. The correspondence is very high and supports the above analysis. In addition, we have calculated the electron densities at the bond critical points around the C_6 ring by using Bader's Quantum Theory of Atoms In Molecule (QTAIM) [20]. These results are shown in Fig. 3. The calculated electron densities are highest between the two shorter C–C ring bonds, C(2)–C(3) = 0.3182 $e^-/bohr^3$ and C(4)–C(5) = 0.3172 $e^-/bohr^3$ which is consistent with the notion of an increase in bond localization at these two bonds.

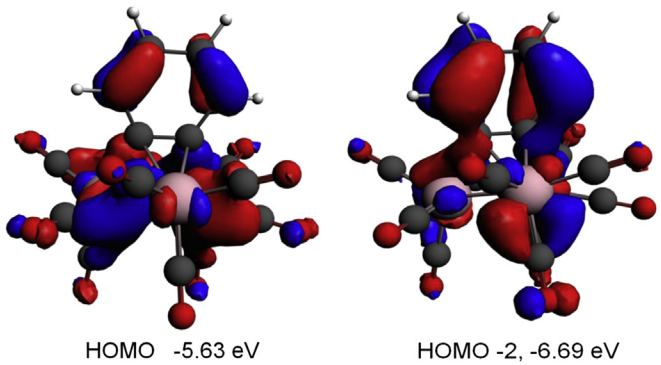

Fig. 2. Molecular Orbital Diagrams of the HOMO and HOMO-2 with their energies for compound **3** showing the π-bonding in the C_6H_4 ring.

Table 2
Selected bond distances for **3** from X-ray and geometry-optimized DFT calculations.

Atoms	Distance Å (X-ray)	Distances Å (DFT)
Os1–Os2	2.8526(3)	2.834
Os2–Os3	2.7506(4)	2.778
Os1–Os3	2.7631(4)	2.775
C1–C2	1.438(9)	1.425
C2–C3	1.375(10)	1.377
C3–C4	1.405(10)	1.413
C4–C5	1.361(10)	1.377
C5–C6	1.428(10)	1.425
C1–C6	1.406(9)	1.438

An ORTEP diagram of the molecular structure of **4** is shown in Fig. 4. Compound **4** contains three osmium atoms, ten CO ligands, one of which is a semi-bridging CO ligand, and two phenyl rings; one of which is σ-bonded to one of the osmium atoms and the other is bonded to a CO group in the form of a bridging benzoyl ligand. The three metal atoms are arranged in a triangle with three Os–Os bonds: Os(1)–Os(2) = 2.8141(7) Å, Os(1)–Os(3) = 2.9020(6) Å, Os(2)–Os(3) = 2.8606(7) Å. The shortest Os(1)–Os(2) bond is the one that contains the semi-bridging CO ligand C(11)–O(11) and the bridging benzoyl ligand: Os(2)–C(1) = 2.087(11) Å, Os(1)–O(1) = 2.129(7) Å and C(1)–O(1) = 1.287(12) Å. The phenyl ligand is terminally coordinated to Os(1), Os(1)–C(4) = 2.125(10) Å. Two other osmium carbonyl cluster complexes containing σ-phenyl ligands, $Os_4(CO)_{15}Ph(\mu_4\text{-Bi})$ with Os – C = 2.178(7) Å and $Os_5(CO)_{19}Ph(\mu_4\text{-Bi})$ with Os – C = 2.152(13) Å, were obtained from the reaction of $BiPh_3$ with $Os_3(CO)_{11}(NCMe)$, see Scheme 1 [13]. Leong obtained some osmium carbonyl cluster complexes containing σ-phenyl ligands by cleaving a phenyl group from a $SbPh_3$ ligand [4].

An ORTEP diagram of the molecular structure of **6** is shown in Fig. 5. Compound **6** contains six osmium atoms in two groups of four and two. The two groups are bridged by a spiro-μ_4-Bi atom, Os(1)–Bi(1) = 2.7644(12) Å, Os(2)–Bi(1) = 2.7085(13) Å, Os(5)–Bi(1) = 2.7203(12) Å and Os(6)–Bi(1) = 2.7235(13) Å. Four compounds containing spiro-μ_4-Bi atoms were obtained in the reaction of $BiPh_3$ in its reaction with $Os_3(CO)_{11}(NCMe)$, Scheme 1 [13]. One of those was the compound **5** which was also obtained in this reaction. The Os–Bi distances in those compounds are similar to those found in **6**. The Os–Os bond distances in **6** are not unusual, except for the elongated Os(5)–Os(6) bond of 3.0309(13) Å in the Os_2 group. This bond is bridged by a hydride ligand which was located and refined crystallographically, Os(5)–H(1) = 1.71(19) Å, Os(6)–H(1) = 2.01(19) Å. The presence of hydride ligand explains the longer Os–Os bond length [23]. The ^{1}H NMR spectrum of freshly dissolved crystals of **6** exhibits a high-field resonance at $\delta = -14.54$, for the hydride ligand; however, a new resonance grows in at $\delta = -14.59$ ppm within a matter of minutes. After about 3 h, the two resonances become almost equal in intensity 48/52 and remain in this ratio thereafter. We interpret this as due to the formation of a second isomer of compound **6** which exists in equilibrium with **6** solution. Efforts to isolate, crystallize and obtain a structural characterization of the isomer having the resonance at −14.59 ppm have been unsuccessful. Compound **6** contains μ-η^2-C_6H_4 ligand bridging the osmium atoms in the two atom group, Os(5)–C(1) = 2.12(3), Os(6)–C(2) = 2.11(3). μ-η^2-C_6H_4 ligands are rare, but one was also found in the compound $HOs_5(CO)_{18}(\mu\text{-}C_6H_4)(\mu_4\text{-Bi})$, **5**, Os(1)-C(2) = 2.110(11) Å, Os(2)-C(1) = 2.132(12) Å which was obtained from the reaction of $Os_3(CO)_{11}(NCMe)$ with $BiPh_3$ [13]. Leong also obtained some examples of μ-η^2-C_6H_4 ligands in some osmium carbonyl cluster complexes formed by the cleavage of phenyl rings from $SbPh_3$ ligands [26]. Except for the C–C bond that bridges the Os(5)–Os(6) bond, C(1)–C(2) = 1.47(3) Å, the C–C bonds in the C_6 ring in **6** are all very similar in length and all are within two estimated standard deviations of each other: C(1)–C(6) = 1.38(3) Å, C(2)–C(3) = 1.41(3) Å, C(3)–C(4) = 1.37(4) Å, C(4)–C(5) = 1.39(4) Å, C(5)–C(6) = 1.40(3) Å. This indicates that, unlike the benzyne ring

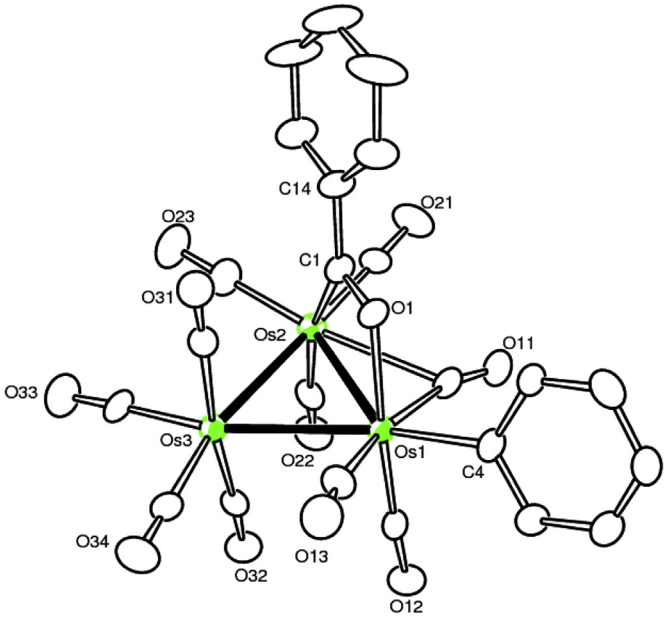

Fig. 4. An ORTEP diagram of the molecular structure of $Os_3(CO)_{10}Ph(\mu\text{-}\eta^2\text{-O=CPh})$, **4** showing 30% thermal ellipsoid probability. The hydrogen atoms are omitted for clarity. Selected interatomic bond distances (Å) are as follow: Os(1)–Os(2) = 2.8141(7), Os(1)–Os(3) = 2.9020(6), Os(2)–Os(3) = 2.8606(7), Os(2)–C(1) = 2.087(11), C(1)–O(1) = 1.287(12), Os(1)–O(1) = 2.129(7), Os(1)–C(4) = 2.125(10), Os(1)–C(11) = 1.957(13), Os(2)–C(11) = 2.615(13).

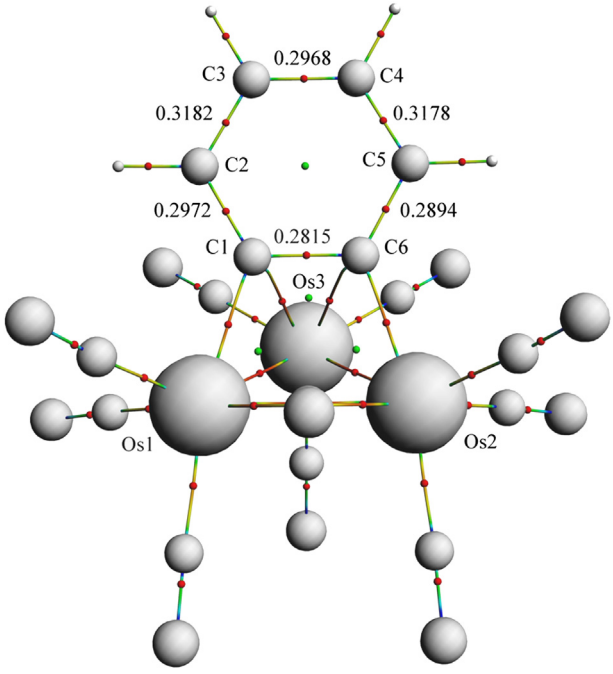

Fig. 3. A drawing of the structure of **3** showing the electron densities at bond critical points in the ring of the benzyne ligand calculated by the QTAIM method by using the DFT optimized structure.

in **3**, any localization in the π-bonding of the benzyne ring in **6** is much smaller than that in **3** and is probably insignificant. The reason for this is because the interactions of the out of plane π-orbitals of the ring with the metal atoms in **6** are much smaller than with those is **3**. The long length of the C(1)–C(2) bond in **6** can be explained by di-σ-bonding of C(1) and C(2) to the two osmium atoms which involves significant π-back bonding to the in plane π-bond at the formal C(1)–C(2) triple of the benzyne ligand. The spiro-Bi atom in **6** acts as a 5-electron donor and thus all of the transition metal atoms in **6** formally have 18 electron configurations.

When compound **4** was heated to reflux in hexane solvent for 5 h, it was transformed into compound **3** in 10.5% yield and the compound $Os_3(CO)_{10}(\mu\text{-}\eta^2\text{-}O{=}CPh)_2$, **7** in 42% yield. Compound **7** was obtained by Kaesz many years ago from the reaction of $Os_3(CO)_{12}$ with phenyl lithium followed by the oxidation with $(Me_3O)(SbCl_6)$ or $CuBr_2$ [15], but this molecule was never characterized structurally by X-ray crystallographic methods. That has been done in this work. An ORTEP diagram of the molecular structure of **7** is shown in Fig. 6. Compound **7** contains a triangular cluster of three osmium atoms with ten linear terminal carbonyl groups and two benzoyl ligand that bridge the atoms Os(1) and Os(2). The benzoyl ligands serve as three electron donors so the metal atoms have a total of 50 valence electrons and thus all of the metal atoms achieve 18-electron configurations with the existence of only two Os–Os bonds. These are Os(1)–Os(3) = 2.8720(6) Å and Os(2)–Os(3) = 2.8810(7) Å. The Os(1)–Os(2) distance of 3.652(1) Å is clearly a nonbonding interaction. The two benzoyl ligands are paired antisymmetrically such that the oxygen atom of one is bonded to Os(1) and the oxygen atom of the other is bonded to Os(2); Os(1)–O(1) = 2.112(6) Å, Os(2)–O(2) = 2.100(7) Å (Fig. 6).

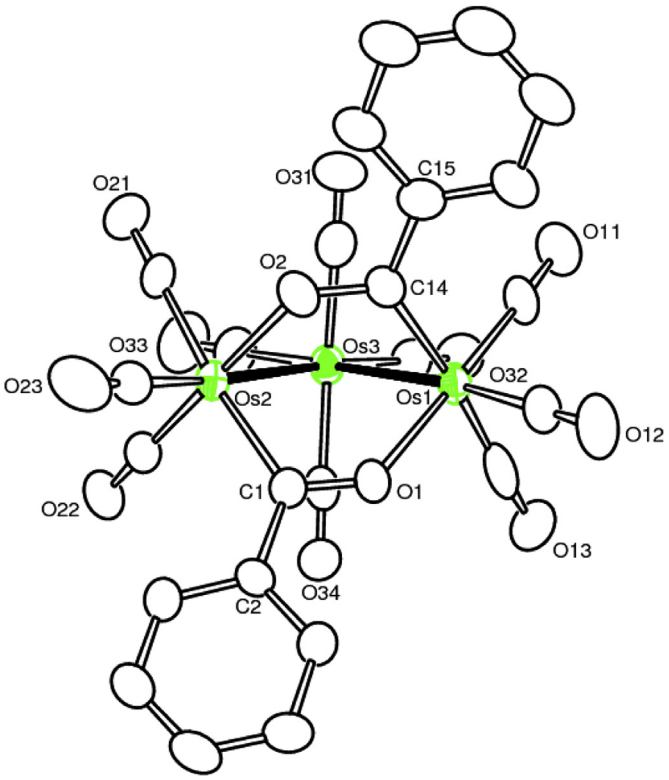

Fig. 6. An ORTEP diagram of the molecular structure of $Os_3(CO)_{10}(\mu\text{-}\eta^2\text{-}O{=}CPh)_2$, **7** showing 30% thermal ellipsoid probability. The hydrogen atoms are omitted for clarity. Selected interatomic distances (Å) are as follow: Os(1)·Os(2) = 3.652(1), Os(1)–Os(3) = 2.8720(6), Os(2)–Os(3) = 2.8810(7), Os(2)–C(1) = 2.086(9), C(1)–O(1) = 1.256(10), Os(1)–O(1) = 2.112(6), Os(1)–C(14) = 2.091(10), C(14)–O(2) = 1.296(11), Os(2)–O(2) = 2.100(7).

5. Discussion

A summary of the reactions and products obtained in this study is shown in the Scheme 2. Five products **2**–**6** were formed from the reaction of **1** with $BiPh_3$. Compounds **5** and **6** contain spiro-μ_4-Bi atoms formed by the cleavage of all of the phenyl groups from the $BiPh_3$. Products **3** and **4** contain the phenyl rings that were cleaved from the $BiPh_3$, although the ring in **3** is actually a triply-bridging C_6H_4 ligand formed by the cleavage and elimination of one hydrogen atom from a phenyl ring. A high quality structural analysis of **3** coupled with a DFT computational analysis indicates that there is a significant degree of localization of the π-bonding in that ring. Compound **3** was also obtained in a low yield by heating **4**. It is

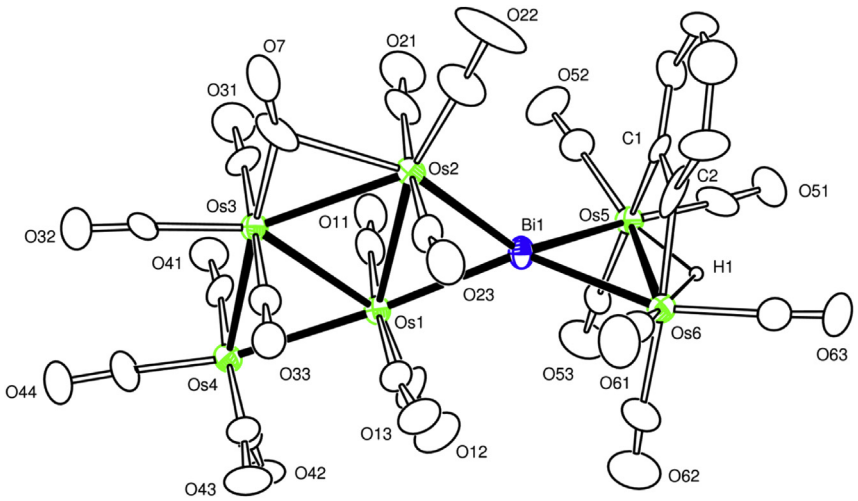

Fig. 5. An ORTEP diagram of the molecular structure of $Os_6(CO)_{20}(\mu\text{-}\eta^2\text{-}C_6H_4)(\mu_4\text{-}Bi)(\mu\text{-}H)$, **6** showing 30% thermal ellipsoid probability. The hydrogen atoms are omitted for clarity. Selected interatomic bond distances (Å) are as follow: Os(1)–Os(2) = 2.9511(13), Os(1)–Os(3) = 2.8875(12), Os(1)–Os(4) = 2.8268(13), Os(2)–Os(3) = 2.8553(13), Os(3)–Os(4) = 2.8972(13), Os(5)–Os(6) = 3.0309(13), Os(1)–Bi(1) = 2.7644(12), Os(2)–Bi(1) = 2.7085(13), Os(5)–Bi(1) = 2.7203(12), Os(5)–H(1) = 1.71(19), Os(6)–H(1) = 2.01(19), Os(6)–Bi(1) = 2.7235(13), Os(5)–C(1) = 2.12(3), Os(6)–C(2) = 2.11(3), C(1)–C(2) = 1.47(3), C(1)–C(6) = 1.38(3), C(2)–C(3) = 1.41(3), C(3)–C(4) = 1.37(4), C(4)–C(5) = 1.39(4), C(5)–C(6) = 1.40(3).

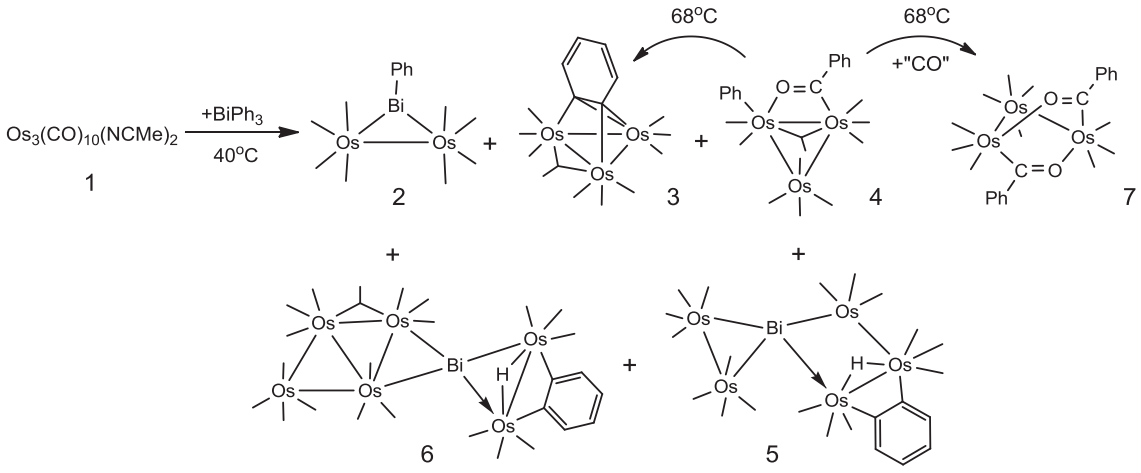

Scheme 2.

anticipated that **3** was formed by the elimination of benzaldehyde from **4**, but that was not confirmed experimentally. The compound **7** was also obtained from the thermal treatment of **4**. The formation of **7** requires formally the addition of an equivalent of CO, presumably provided by small amounts of CO formed by degradation of some of the **4** and then a coupling of the CO to the phenyl group to produce the second benzoyl ligand found in **7**.

6. Conclusions

The cleavage of phenyl groups from $BiPh_3$ by activated osmium carbonyl cluster complexes is facile and leads to products containing naked bridging bismuth atoms and coproducts containing the phenyl rings. Similar results were found in our studies of the reactions of $BiPh_3$ with activated rhenium carbonyl complexes [11]. Evidence has been presented that shows a pattern of alternating long and short C–C distances in the bridging benzyne ligand in **3** that is consistent with a significant amount of localization in π-bonding in the ring that is induced by the coordination of the triple bond of the ring to the metal atoms.

Acknowledgments

This research was supported by the National Science Foundation under grants No. CHE-1111496 and CHE-1048629 for the purchase of the computational facility.

Appendix A. Supplementary material

CCDC 938624, 938625, 938626 and 938627 contain the supplementary crystallographic data for this paper. These data can be obtained free of charge from The Cambridge Crystallographic Data Centre via www.ccdc.cam.ac.uk/data_request/cif.

Appendix B. Supplementary data

Supplementary data related to this article can be found at http://dx.doi.org/10.1016/j.jorganchem.2013.07.027.

References

[1] C.W. Bradford, R.S. Nyholm, G.J. Gainsford, J.M. Guss, P.R. Ireland, R. Mason, J. Chem. Soc. Chem. Commum. (1972) 87–89.
[2] G.J. Gainsford, J.M. Guss, P.R. Ireland, R. Mason, C.W. Bradford, R.S. Nyholm, J. Organomet. Chem. 40 (1972) C70–C72.
[3] C.T. Tay, W.K. Leong, J. Organomet. Chem. 625 (2001) 231–235.
[4] W.K. Leong, G. Chen, Organometallics 20 (2001) 2280–2287.
[5] H. Braunschweig, P. Cogswell, K. Schwab, Coord. Chem. Rev. 255 (2011) 101–117.
[6] K.H. Whitmire, J. Cluster Sci. 2 (1991) 231–258.
[7] T.A. Hanna, Coord. Chem. Rev. 248 (2004) 429–440.
[8] R.K. Grasselli, J.D. Burrington, D.J. Buttrey, P. DeSanto Jr., C.G. Lugmair, A.F. Volpe Jr., T. Weingand, Top. Catal. 23 (2003) 5–22.
[9] W.A. Goddard III, K. Chenoweth, S. Pudar, A.C.T. van Duin, M.-J. Cheng, Top. Catal. 50 (2008) 2–18.
[10] R.D. Adams, B. Captain, W.C. Pearl Jr., J. Organomet. Chem. 693 (2008) 1636–1644.
[11] R.D. Adams, W.C. Pearl Jr., Inorg. Chem 48 (2009) 9519–9525.
[12] R. Raja, R.D. Adams, D.A. Blom, W.C. Pearl Jr., E. Gianotti, J.M. Thomas, Langmuir 25 (2009) 7200–7204.
[13] R.D. Adams, W.C. Pearl Jr., Inorg. Chem. 49 (2010) 7170–7175.
[14] D. Braga, F. Grepioni, E. Parisini, B.F.G. Johnson, C.M. Martin, J.G.M. Nairn, J. Lewis, M. Martinelli, J. Chem. Soc. Dalton Trans. (1993) 1891–1895.
[15] C.M. Jensen, Y.-J. Chen, C.B. Knobler, H.D. Kaesz, New J. Chem. 12 (1988) 649–660.
[16] SAINT+ Version 6.2a, Bruker Analytical X-ray System, Inc., Madison, Wisconsin, USA, 2001.
[17] G.M. Sheldrick, SHELXTL Version 6.1, Bruker Analytical X-ray Systems, Inc., Madison, Wisconsin, USA, 1997.
[18] ADF2012, Scm Theoretical Chemistry, Vrije Universiteit, Amsterdam, The Netherlands, 2012, http://www.scm.com.
[19] J.P. Perdew, A. Ruzsinszky, G.I. Csonka, O.A. Vydrov, G.E. Scuseria, Phys. Rev. Lett. 100 (2008) 136406.
[20] (a) R.F.W. Bader, Atoms in Molecules: a Quantum Theory, Clarendon, Oxford, 1990;
(b) F. Cortés-Guzmán, R.F.W. Bader, Coord. Chem. Rev. 249 (2005) 633–662.
[21] AIMAll, Version 12.11.09, T.A. Keith, Tk Gristmill Software. Overland Park KS, USA, 2012, aim.tkgristmill.com.
[22] R.J. Goudsmit, B.F.G. Johnson, J. Lewis, P.R. Raithby, M.J. Rosales, J. Chem. Soc. Dalton Trans. (1983) 2257–2261.
[23] R. Bau, M.H. Drabnis, Inorg. Chim. Acta 259 (1997) 27–50;
(b) R.G. Teller, R. Bau, Struc. Bonding 41 (1981) 1–82.
[24] (a) S. Deabate, R. Giordano, E. Sappa, J. Cluster Sci. 8 (1997) 407;
(b) A. J.Deeming, Adv. Organomet. Chem. 26 (1086) 1.
[25] M.R. Hassan, S.E. Kabir, B.K. Nicholson, E. Nordlander, Md. Nazim Uddin, Organometallics 26 (2007) 4627–4633.
[26] G. Chen, M. Deng, C.K.D. Lee, W.K. Leong, J. Tan, C.T. Tay, J. Organomet. Chem. 691 (2006) 387–394.